

Two-dimensional coarsening and phase separation in thin polymer solution films

Christopher K. Haas¹ and John M. Torkelson^{1,2,*}

¹*Department of Chemical Engineering, Northwestern University, Evanston, Illinois 60208-3120,*

²*Department of Materials Science and Engineering, Northwestern University, Evanston, Illinois 60208-3120*

(Received 21 March 1996; revised manuscript received 11 October 1996)

A comprehensive experimental study on the late stages of phase separation in two dimensions was performed by phase separating thin (1.5 and 10 μm) films of off- and near-critical polymer solutions. The resulting domain-size growth rate (coarsening rate) of the dispersed phase was directly measured for several systems using optical microscopy. Domain sizes of off-critical solutions coarsen predominantly via Ostwald ripening, growing approximately as $Kt^{1/3}$, regardless of system. For near-critical solutions, domain sizes grow approximately as $Kt^{1/3}$ at early times, with coarsening via both coalescence and Ostwald ripening, and feature a crossover to an ultimate $t^{2/3}$ growth rate. The crossover domain size decreases with increasing quench depth in a manner consistent with a transition from a thermally driven to a flow-driven coarsening mechanism. In general, K increases with area fraction of the dispersed phase for a given off-critical or near-critical system. Both average and crossover domain sizes increase with increasing film thickness, and coalescence is significantly dependent on film thickness while Ostwald ripening is not. The substrate polarity does not greatly affect off-critical coarsening, although near-critical coarsening (particularly near the crossover) is greatly affected. Other effects of polymer molecular weight, solvent viscosity, and quench depth are discussed. [S1063-651X(97)13303-7]

PACS number(s): 61.25.Hq, 61.41.+e, 64.75.+g, 68.55.-a

INTRODUCTION

The dynamics of binary liquid-liquid phase separation in various geometries has received much attention recently [1–23], in particular, the later stages of phase separation where the domains of the minority phase grow according to a power law t^α , where t is the coarsening time and α is the growth-rate exponent. One aspect of liquid-liquid phase separation that differs from phase separation in metallic alloys is the presence of flow, which strongly affects the domain growth [1]. The effects of this flow behavior have been well described theoretically [1,5] and experimentally [6–10] for three-dimensional (3D) systems; however, to date the effects of flow on two-dimensional (2D) coarsening have been the subject of relatively little experimental study. This will be the first comprehensive experimental investigation of 2D coarsening dynamics, to our knowledge.

When a homogeneous solution is quenched into the two-phase region of its phase diagram to a temperature T_{PS} , two phases will form. For the binary polymer-solvent systems studied here, polymer-rich and polymer-lean phases will form. The relative amounts of each phase are related to the quench depth (ΔT is the distance from the binodal curve) and the distance and direction from the critical composition (ϕ_c). For example, the polymer-lean phase of a system phase separated from a solution with less-than-critical composition is the majority (matrix) phase, and the rich phase is the minority (dispersed) phase. The converse is not necessarily true for a solution with greater-than-critical composition due to the asymmetric nature of some polymer-solvent phase diagrams. Often, the two phases reach their equilibrium compositions relatively quickly; however, the system is not at equilibrium.

The high interfacial area between the phases causes a high interfacial energy which is dissipated in a process known as coarsening [11].

There are three main coarsening mechanisms described for 3D systems that have been applied to 2D systems, and in each case it is assumed that the two phases have reached their equilibrium compositions. In the Ostwald ripening mechanism, two assumptions are made: the area fraction of the dispersed phase F_A is small, and the chemical potential of a coarsening droplet is directly proportional to its curvature [11]. Based on this second assumption, smaller particles (with high curvature) are unstable, and larger particles tend to grow by dissolution of the smaller particles in an evaporation-condensation mechanism. The average domain size (d) of the dispersed phase for 2D Ostwald ripening has been theoretically and numerically predicted [12] to grow as $Kt^{1/3}$. The parameter K has been predicted to be mildly dependent on the interfacial tension between the phases (σ), T_{PS} , the diffusion constant, and other materials parameters [13]. K has also been predicted to be strongly dependent on F_A [11]; as F_A increases, interparticle interactions increase and diffusional length scales decrease, resulting in an increase in K .

For sufficiently large F_A (i.e., for near-critical systems), impingement of droplets brought together by Brownian motion, or coalescence, becomes important. Recent predictions for the 2D domain-size growth-rate exponents in this second coarsening regime range from $\frac{1}{4}$ [14] to $\frac{1}{3}$ [15] to $\frac{1}{2}$ [1,16] at early times, and for liquid-liquid systems feature a crossover to the third coarsening regime, hydrodynamic flow. In this regime, pressure gradients due to σ effects become more important than curvature or thermal effects. In an interconnected phase, there are several different length scales, with “narrow” regions between closely spaced droplets of the other phase and “wide” regions between spatially distant

*Author to whom correspondence should be addressed.

droplets. There are pressure differences between narrow and wide regions due to interfacial tension. Since the interconnected phase is a liquid, there will be material flow from narrow regions to wide regions. This flow, known as hydrodynamic flow, accelerates coarsening; the domain-size growth rate for this mechanism was analyzed for a 3D geometry by Siggia [5], who predicted an ultimate t^1 growth rate. More recently, a more thorough scaling analysis was performed on 2D and 3D systems by Furukawa [1,17]. For flow-dominated coarsening in phase-separated systems, Furukawa [1] predicted the ultimate domain-size growth rates for 2D and 3D coarsening by scaling the coupled Navier-Stokes and Cahn-Hilliard equations; he also included inertial effects which were ignored in previous scaling analyses. He predicted two growth rates for flow-dominated 3D coarsening in the absence of gravitational effects, $d \sim t^1$ followed by $d \sim t^{2/3}$, and only one for 2D flow-dominated coarsening, $d \sim t^{2/3}$. He claimed that the ultimate $t^{2/3}$ growth rate is due to the balance of interfacial tension and inertial forces. The penultimate t^1 growth rate predicted to occur in 3D systems is not observed in 2D systems because the dissipative forces that balance the interfacial tension forces for 3D systems are not allowed in the 2D case. This $t^{2/3}$ growth rate for 2D systems has since been verified by several numerical studies [14,15,18] and one experimental study [19].

A primary experimental difficulty in studying 2D coarsening is the preferential wetting of one phase on the sample cell walls [20]. Differences between σ for the liquid-liquid and liquid-solid phases in thin-layer phase separated systems cause curvature between the phases. For shallow-quenched critical phase-separated systems in such a geometry, σ between the two liquid phases and the solid phase may result in one of the liquid phases forming a wetting layer over the entire substrate surface. This complete covering of the substrate by one phase is known as critical wetting [24]. Bodensohn and Goldburg [20] claimed that a wetting layer in their phase-separated thin (100- μm gap) 2,6-lutidine-water solutions accelerated coarsening over much of the time frame studied. Despite the potential complications this phenomenon presents to studying 2D coarsening, there are advantages to studying coarsening in thin films. When studying 3D coarsening, it may be necessary to use extraordinarily shallow quenches (especially for small molecule systems [6]), very viscous systems (such as a polymer blends [7,8,25]), or isodensity (isopycnic) systems [9,10,26] in order to delay macroscopic phase separation caused by gravity. Gravity effects are negligible in a 2D geometry; therefore, these precautions are unnecessary. In addition, phase separation and coarsening in a 2D geometry may be directly viewed by optical microscopy, unlike many of the more indirect methods used in 3D studies. Some recent studies have attempted to examine 3D coarsening using "direct" techniques such as optical microscopy [27–29] or confocal microscopy [30]; however, there is significant droplet overlap in the former studies and few data points due to experimental complexity in the latter study, difficulties not encountered when studying 2D coarsening by optical microscopy.

Despite these advantages, there are very few successful experimental 2D coarsening studies presented in the literature [19,20,31–33], and they are all limited in nature; only one [19] reported domain-size growth rates for more than

TABLE I. Approximate critical temperatures (T_c) and critical compositions (ϕ_c) for the polymer-solvent systems used in this study.

	300 kPS- DEO	2000 kPS- DEO	2000 kPS- DEM	300 kPS- DIDP
T_c ($^{\circ}\text{C}$)	36.5	48	28.5	60
ϕ_c (wt %)	6	3	5	8

one system. In that study, rates for off-critical and near-critical polystyrene (PS)–diethyl oxalate (DEO) systems were reported, with off-critical domains growing as approximately $t^{1/3}$ at early times and accelerating to an apparent $t^{2/3}$ growth rate at longer times. The current study will present more comprehensive results by demonstrating the dependence of 2D coarsening on a variety of system parameters, including polymer molecular weight, solvent, composition, quench depth, and film thickness (gap width).

DESCRIPTION OF EXPERIMENTS

Two relatively monodisperse PS standards (Pressure Chemical) and solvents diethyl malonate (DEM, Aldrich) and diisodecyl phthalate (DIDP, TCI-Chemical) were used as received. As it is highly hygroscopic, the solvent DEO (Aldrich) was dried prior to use by adding anhydrous potassium carbonate, and DEO solutions were prepared and stored under a nitrogen atmosphere in order to prevent water uptake. The lower molecular weight PS standard (300kPS) had a number average molecular weight, M_n , of 2.9×10^5 with a polydispersity (M_w/M_n , where M_w is the weight average molecular weight) of 1.06. M_n for the higher molecular weight PS standard (2000kPS) was 2.0×10^6 ; the polydispersity was 1.2. Phase diagrams were determined from turbidimetry as described elsewhere [34]. The critical temperatures (T_c) indicated in Table I are slightly above room temperature, facilitating easy handling of the solutions.

Homogeneous solutions were sandwiched between two microscope slides maintained at a constant gap width by monodisperse glass beads (Duke Scientific). The beads were placed far from the viewing area (>1 cm) so as not to influence the phase separation or coarsening. Two different substrates (glass and nonpolar) and two bead diameters (1.5 and 10 μm) were used. The nonpolar slides were prepared by chemically depositing dimethyl siloxane on glass slides using a procedure outlined elsewhere [35]. The samples were placed in a Mettler hot stage and quenched at $2^{\circ}\text{C}/\text{min}$ to the desired phase separation temperature. Samples which were quenched too quickly ($>4^{\circ}\text{C}/\text{min}$) featured strong temperature gradients, and samples quenched too slowly ($<0.5^{\circ}\text{C}/\text{min}$) featured strong concentration gradients; these gradients produced unusual, nonregular morphologies. The measurement of coarsening time was started as soon as phase separated structures could be observed through the optical microscope (Nikon Optiphot2.pol); equipment limitations allow accurate domain size determination when $4 \leq d \leq 60$ μm . Since phase separation began before temperature equilibrium had been reached, domain sizes were measured only after several minutes had elapsed. Thus it can be safely as-

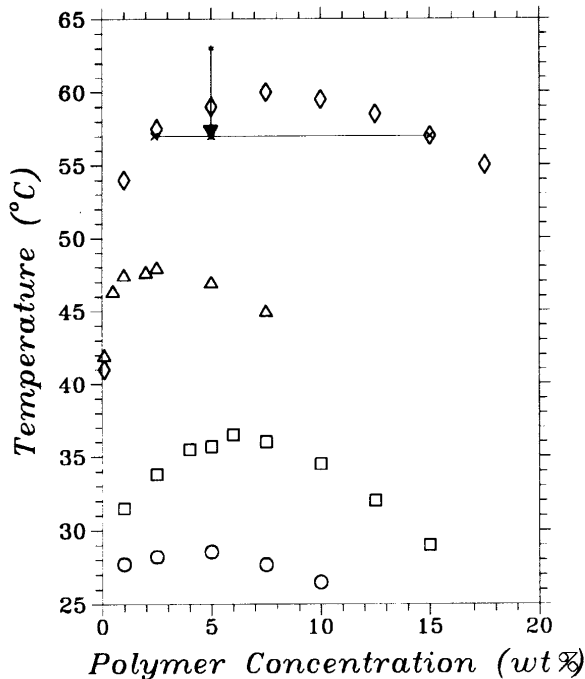


FIG. 1. Cloud point curves (phase diagrams) for all four systems used in this study. \square : 300kPS-DEO; \triangle : 2000kPS-DEO; \circ : 2000kPS-DEM; \diamond : 300kPS-DIDP. The quench shown is for 5 wt % 300kPS-DIDP ($\Delta T=2^\circ\text{C}$), which from the tie line gives an area fraction of the dispersed phase (F_A) of ~ 0.20 .

sumed that the early stages of phase separation were complete (F_A was constant) prior to taking coarsening data for each of the regular systems described here, i.e., the noncritical systems, and that samples had reached final temperature.

RESULTS AND DISCUSSION

General coarsening behavior

Phase diagrams for the PS-solvent systems are given in Fig. 1, and the approximate T_c and ϕ_c values are given in Table I. For almost all of the systems studied, relatively shallow quenches were performed ($\Delta T \leq 4^\circ\text{C}$); the phase diagrams for the 300kPS systems are nearly symmetric for these shallow quenches, i.e., a critical quench results in $F_A \approx 0.5$. Other observed values follow the tie lines as predicted, e.g., for a 5 wt % 300kPS-DIDP solution quenched 2°C ($\Delta T = 2^\circ\text{C}$) into the two-phase region (to $T_{PS} = 55^\circ\text{C}$), the expected F_A value based on the tie line in Fig. 2 is approximately 0.20, equivalent to the F_A value determined from the optical micrograph. It should be noted that for the 2000kPS systems significant asymmetry is present in the phase diagrams at all but the smallest quenches.

Typical micrographs following the coarsening of an off-critical system are given in Fig. 2(a); the average domain size of the dispersed phase (d) for such a circular morphology was taken to be the average circle diameter. Since d was generally of the order of or larger than the gap width and no overlap between droplets was observed for the coarsening times studied, the observed circles can be thought of as disks instead of spheres; thus the domain growth can be considered to be 2D coarsening. The morphology of near-critical systems was similar to that of off-critical systems [see Fig. 2(a)], except with larger F_A values. For all off- and near-critical systems studied, F_A values were approximately constant over the time frame studied, indicating that the phases had reached their equilibrium compositions prior to domain size measurement.

Approximately critical systems featured very irregular morphologies [see Fig. 2(b)] and apparently extremely fast

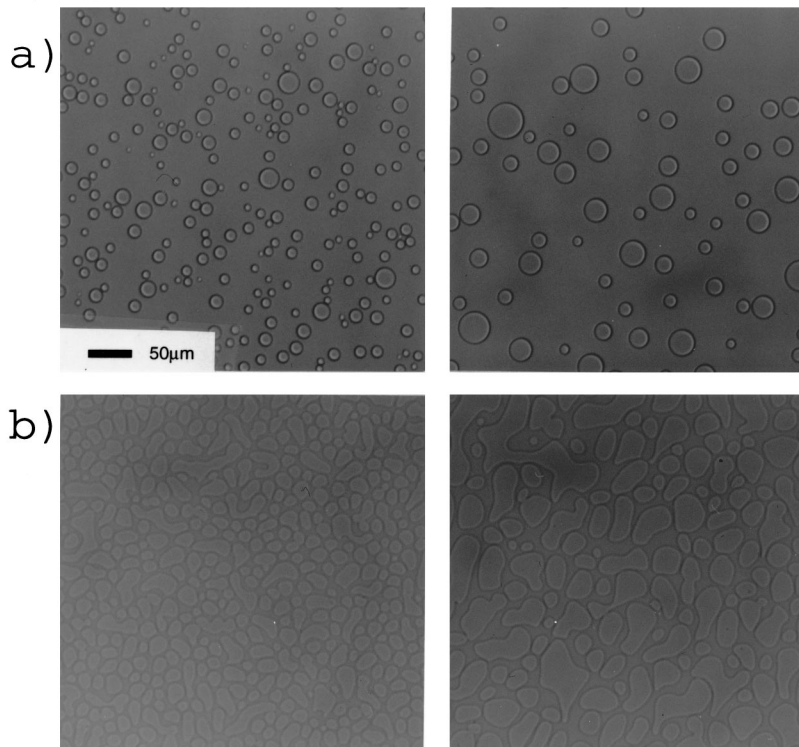


FIG. 2. Optical micrographs for PS-DEO solutions using a $10\text{-}\mu\text{m}$ gap width between glass slides: (a) 300kPS-DEO, 2.5 wt % (off-critical), quench depth (ΔT)= 2°C , coarsened for 1440 s (left) and 10 000 s (right). (b) 300kPS-DEO, 6.0 wt % (critical), $\Delta T=2^\circ\text{C}$, coarsened for 60 s (left) and 120 s (right). Please note the growth of domains (i.e., circles) with time and the difference between the off-critical (circular) and critical (irregular) morphologies. The scale bar is applicable to all four micrographs.

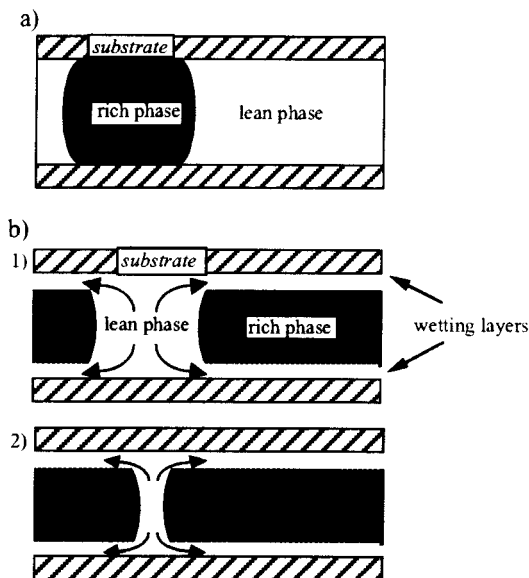


FIG. 3. Schematics of cross section of phase-separated 2D sample. (a) The schematic for the polymer-lean solution cross section in which the rich phase is the dispersed phase. (b) The schematic for the polymer-rich solution, where the lean phase is the dispersed phase and when (1) the domain size of the lean phase is of the order of the gap width; and (2) some later time, where the lean phase domains are being “squeezed” along wetting layers.

coarsening rates ($d > t^1$) from which domain sizes could not be accurately determined; this behavior was observed before in a study of 2D coarsening of a critical composition of 2,6-lutidine–water by Bodensohn and Goldberg [20], who attributed it to the formation of a wetting layer. It is possible that since a wetting layer by one phase would allow greater interconnectivity between phases, the additional diffusional degree of freedom could enable flow effects and a faster growth rate. This additional flow, which occurs while the phases are reaching their equilibrium compositions, is most likely the cause of the unusual morphologies. This theory is validated both by the nonconstant F_A values for these critical systems, implying that the phase compositions are not constant and/or that there are shrinking wetting layers [20], and by the fast growth rate, which is possible when these extra diffusion driving forces are present. Due to the complexity of the morphologies, from which quantitative domain size values could not be measured, critical coarsening behavior will not be discussed further here.

Only less-than-critical (polymer-lean) compositions of these systems could be studied quantitatively in a 2D geometry. Coarsening in phase-separated polymer-rich solutions stopped once the average domain size of the dispersed phase approached the gap width; the dispersed phase domains then appeared to “dissolve” (i.e., the dispersed-phase domain size decreased with time) until only matrix phase remained over most of the sample. Coarsened structures were only present near the edges at much higher than predicted F_A values; therefore, the minority polymer-lean phase, after its apparent dissolution, traveled over the relatively large distance to the sample edges. This behavior may have been caused by the formation of a wetting layer. Since the glass slide prefers the more polar polymer-lean phase over the less

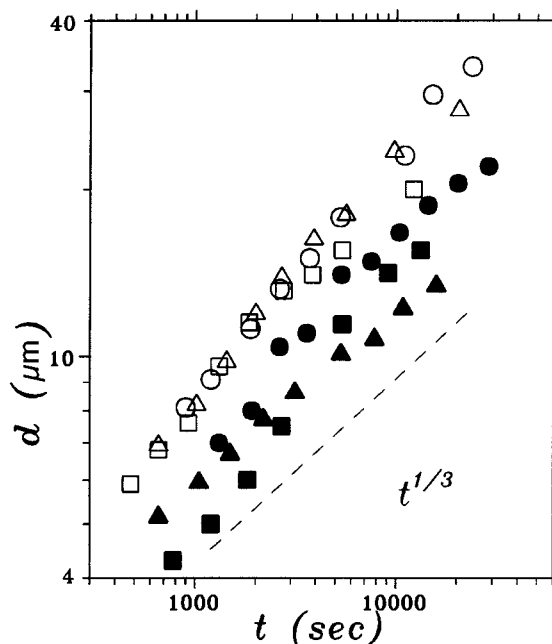


FIG. 4. Average domain size (d) of the minority phase as a function of coarsening time for several off-critical solutions phase separated between glass slides with a 10- μm gap width. \blacktriangle : 2.5 wt % 300kPS-DEO, $\Delta T=1^\circ\text{C}$, $F_A\sim 0.11$; \triangle : 2.5 wt % 300kPS-DEO, $\Delta T=2^\circ\text{C}$, $F_A\sim 0.16$; \square : 1.0 wt % 2000kPS-DEO, $\Delta T=4^\circ\text{C}$, $F_A\sim 0.11$; \blacksquare : 1.0 wt % 2000kPS-DEM, $\Delta T=1^\circ\text{C}$, $F_A\sim 0.10$; \circ : 5.0 wt % 300kPS-DIDP, $\Delta T=2^\circ\text{C}$, $F_A\sim 0.20$; \bullet : 5.0 wt % 300kPS-DIDP, $\Delta T=4^\circ\text{C}$, $F_A\sim 0.20$. The slope is not a fit, only a guide.

polar polymer-rich phase, a contact angle between the two liquid phases and the solid phase is formed, causing a curvature between the two liquid phases. This is shown schematically for a majority lean-phase system in Fig. 3(a). If the more mobile polymer-lean phase is the minority phase, as is the case for shallow-quenched systems with an initial composition greater than ϕ_c , then this curvature acts to “squeeze” the lean phase along a wetting layer to the edges where the interfacial tension would be favorable [see Fig. 3(b)]. The use of nonpolar substrates was unsuccessful in overcoming this difficulty since their use actually *accelerated* this “reversal,” apparently, the additional pressure on the solvent-rich phase by the nonpolar walls forced that phase to diffuse preferentially to the edges, even though the wetting mechanism was not possible.

Off-critical coarsening

Domain-size growth-rate data are shown for several off-critical systems in Fig. 4. Regardless of system, d grows approximately as $t^{1/3}$ (“best-fit” exponents range from 0.34 to 0.42 for the systems in Fig. 4) for the range of domain sizes studied. Changing the solvent from the low viscosity DEO or DEM (viscosity ≈ 2 cP at 25°C for each [29]) to the relatively viscous DIDP (viscosity ≈ 80 cP at 25°C [36]) does not significantly affect the coarsening rate, as evidenced by the significant overlap of data in the DEO and DIDP systems. Similarly, polymer molecular weight and quench depth ΔT had no effect on the growth-rate exponent, although effects of ΔT on domain size at a given coarsening

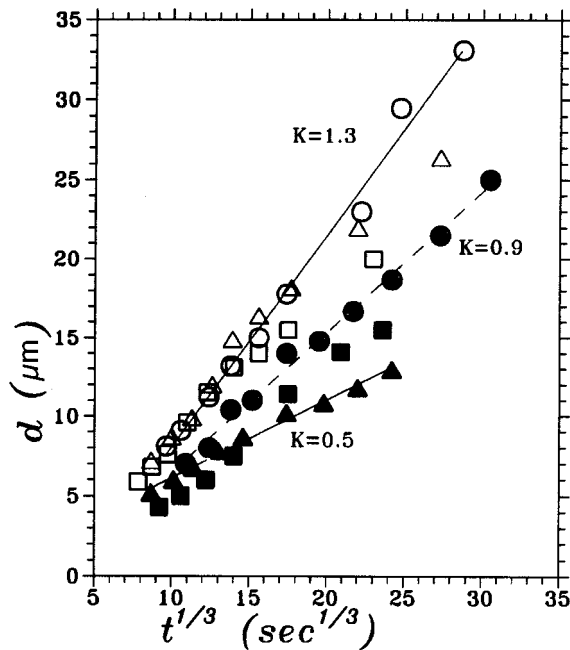


FIG. 5. Plot of d as a function of $t^{1/3}$ for the off-critical systems shown in Fig. 4. The best-fit slopes ($K [=] \mu\text{m/s}^{1/3}$) are also given for three of the systems.

time were substantial. For example, in the case of the 5.0 wt % 300kPS-DIDP system, quench depths of 2 and 4 °C both yielded approximately the same dispersed-phase area fraction F_A of 0.20; under these conditions, increasing the quench depth resulted in smaller d values. This is in accord with expectations based on the initial phase separation mechanism of spinodal decomposition. Before coarsening begins, the fluctuation wavelength, proportional to initial domain size, decreases with increasing ΔT [37]. Thus, as long as the coarsening-rate exponent is system independent for off-critical cases and the growth-rate parameter K is a function of F_A for a given system [11], the observed trend in d values for the 5.0 wt % 300kPS-DIDP is expected. (This assumes that coarsening initiates at sufficiently short times as to appear nearly independent of quench depth on the time scales shown in Fig. 4.) On the other hand, when an increase in quench depth results in a sizable change in F_A , as in the case of the 2.5 wt % 300kPS-DEO system shown in Fig. 4, larger d values may be obtained with the deeper quench, larger F_A system; this indicates the important role played by F_A in affecting the coarsening growth rate through the parameter K .

In order to assess more clearly the effect of F_A on the coarsening growth-rate parameter K , d values were replotted as a function of $t^{1/3}$ for all of the systems in Fig. 5. (An additional reason for plotting data in this manner is that a recent study has shown that determining growth-rate exponents by log-log plots is less appropriate than plotting domain size as a function of time raised to a presumed growth-rate exponent [38].) Figure 5 shows good linearity in all cases, making clear that data yielding an apparent “best-fit” growth-rate exponent slightly above $\frac{1}{3}$ can in fact be fully consistent within experimental error of the expectations an exponent of $\frac{1}{3}$ based on Ostwald ripening theory [12]. (While the exponent of $\frac{1}{3}$ is also consistent with expectations based

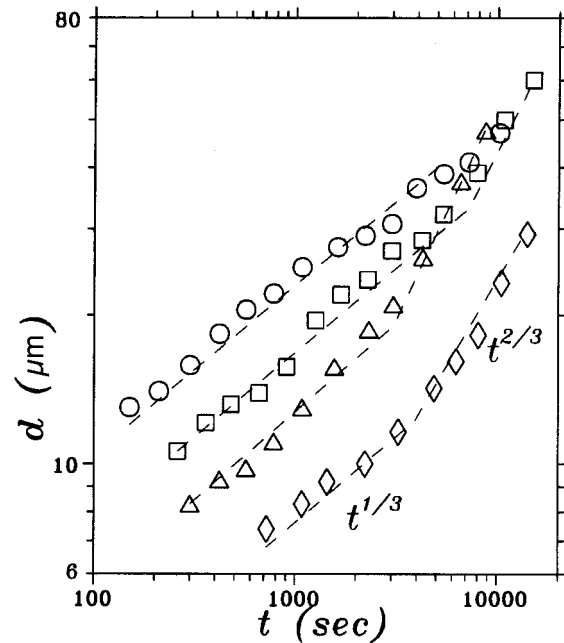


FIG. 6. Temporal dependence of d for near-critical 5 wt % 300kPS-DEO solutions with glass substrates and gap widths of 10 μm : \circ : $\Delta T=1$ °C; \square : $\Delta T=2$ °C; \triangle : $\Delta T=4$ °C; \diamond : $\Delta T=6$ °C. The slopes are not fits, only guides.

on a coalescence mechanism, very little coalescence was observed in off-critical systems; instead smaller droplets were observed to decrease in size while larger droplets increased in size, indicating that the dominant coarsening mechanism was Ostwald ripening.) The parameter K (see slope in Fig. 5) ranges from 0.5 to 1.3 $\mu\text{m/s}^{1/3}$, depending on system and coarsening conditions. For the 2.5 wt % 300kPS-DEO system, an increase in quench depth ΔT from 1 to 2 °C increases the dispersed-phase area fraction from 0.11 to 0.16, resulting in a doubling of K from 0.5 to 1.0 $\mu\text{m/s}^{1/3}$. This increase in K is qualitatively, although not quantitatively, consistent with expectations based on recent theoretical developments [11] indicating that K increases as $F_A^{1/2}$. Somewhat surprisingly, domain-size data taken for a 300kPS-DIDP system at approximately the same F_A but different quench depths (2 and 4 °C) yielded substantially different K values (1.3 and 0.9 $\mu\text{m/s}^{1/3}$, respectively). As will be seen in subsection C, when similar conditions apply in a near-critical coarsening study, K values remain approximately constant as long as F_A also remains approximately independent of quench depth, in accord with expectation from theory. The reason for the singular disagreement with expectations from theory of the 300kPS-DIDP system in off-critical coarsening is not clear at present.

Near-critical coarsening

For the systems studied here, coarsening in most of the near-critical systems is distinctly different from the off-critical case. Droplets are observed to coalesce much more frequently, although coarsening by Ostwald ripening remains significant. While the added coalescence does not alter the early-time growth-rate exponent, the growth rate in the later stage of coarsening is markedly different. Figure 6 shows domain-size growth rates for four near-critical 5 wt %

300kPS-DEO systems quenched to different temperatures. F_A was constant over the time frame studied for all systems ($F_A \approx 0.35$ for all but the $\Delta T = 6^\circ\text{C}$ quench, where $F_A \approx 0.30$), signifying that the phases had reached equilibrium compositions. For the most shallow quench ($\Delta T = 1^\circ\text{C}$), $d \sim t^{1/3}$ over the entire time range studied. However, for a slightly deeper quench (2°C) there is an apparent crossover at $d \approx 30 \mu\text{m}$ to an accelerated coarsening rate. A crossover is more apparent and occurs at a smaller domain size ($d \approx 19 \mu\text{m}$) for the 4°C quench and at an even smaller size ($d \approx 10 \mu\text{m}$) for the 6°C quench. The ultimate growth-rate exponent is $\frac{2}{3}$ (best-fit exponents after the crossover range from 0.62 to 0.69), in agreement with 2D theoretical and numerical studies which include hydrodynamic effects [1,17,18].

The best-fit growth-rate exponents for the early-stage coarsening in near-critical systems range from 0.30 to 0.38, independent of ΔT , similar to the off-critical case. However, domain size decreases with quench depth (see Fig. 6): at a 600-s coarsening time, $d \approx 20 \mu\text{m}$ for $\Delta T = 1^\circ\text{C}$ while $d \approx 9 \mu\text{m}$ for $\Delta T = 4^\circ\text{C}$. The effect of quench depth on domain size is due to the initial phase separation mechanism, spinodal decomposition, as described in subsection B. Thus, if the onset of coarsening occurred at sufficiently short time so that on the long time scales of Fig. 6 they appeared to be nearly independent of quench depth, d values would always be smaller for deeper quenches as long as the parameter K and growth-rate exponent were invariant with quench depth (or in the case of K decreased with quench depth).

This point was evaluated in Fig. 7, which plots the pre-crossover data from Fig. 6 as a function of $t^{1/3}$. The data yield very good linear relationships, with the slopes being the same for the three shallower quenches ($K \approx 2.0 \mu\text{m/s}^{1/3}$) which have approximately the same F_A values (0.35). The slope was lower ($K \approx 0.7 \mu\text{m/s}^{1/3}$) for the deepest quench with the smaller F_A value (0.30). It is interesting to note that although coalescence played some role in coarsening of these near-critical systems, these quench depth results are in qualitative agreement with the dependence of K on dispersed-phase area fraction suggested by Ostwald ripening theory [11], as mentioned in subsection B.

The fact that quench depth affects the domain size at which a crossover in coarsening mechanism and growth rate occurs in near-critical systems (see Fig. 6) may be related to interfacial tension effects. Since interfacial tension between the phases, σ , increases with increasing distance from the critical temperature ($T_c - T_{PS}$), and thus with increasing distance from the binodal curve (ΔT) the crossover domain size decreases with increasing σ . This is in qualitative agreement with Siggia's scaling analysis of 3D systems [5] which predicts that crossover domain size scales as $\sigma^{-1/2}$. However, the agreement is likely not quantitative. For some phase-separated polymer solutions [39], it has been predicted and experimentally determined that $\sigma \sim (1 - T_{PS}/T_c)^{1.25}$. This implies that if Siggia's analysis holds in 2D coarsening, then crossover domain size should scale as $(T_c - T_{PS})^{-0.63}$, a much weaker dependence than actually observed. A more critical study would result when measurements of σ (currently underway in our group via the sessile drop technique [39]) are compared to an analysis specifically considering a 2D geometry. In any case, our crossover behavior is consis-

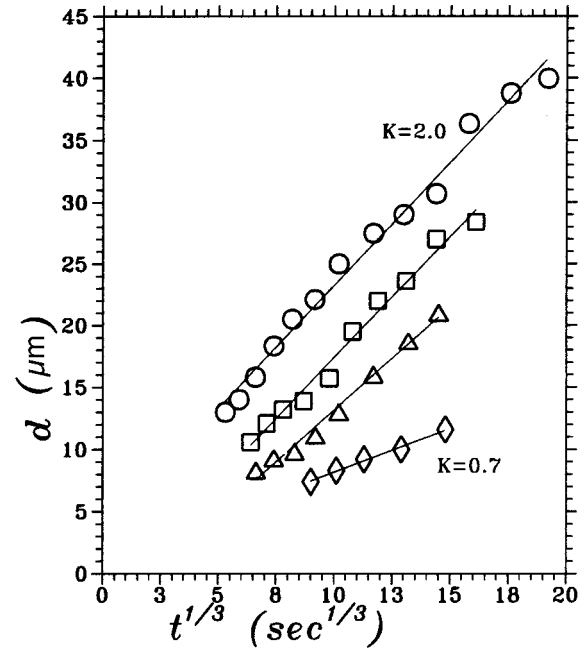


FIG. 7. Plot of d as a function of $t^{1/3}$ for four 5.0 wt % 300kPS-DEO (near-critical) solutions of d values during $\sim t^{1/3}$ growth rate (precrossover), $F_A \sim 0.35$ unless otherwise noted: \circ : $\Delta T = 1^\circ\text{C}$; \square : $\Delta T = 2^\circ\text{C}$; \triangle : $\Delta T = 4^\circ\text{C}$; \diamond : $\Delta T = 6^\circ\text{C}$ ($F_A \sim 0.30$). Note that the lines are best-fit slopes ($K [=] \mu\text{m/s}^{1/3}$).

tent with a crossover from a thermally controlled to an interfacial-tension-controlled (flow-dominated) coarsening mechanism.

Experimental observation of near-critical crossover behavior in 2D phase separation has been reported only once before [19], and for that case, as in this one, the dispersed phase featured a circular morphology. A common misconception is that an "interconnected" morphology is necessary for flow-dominated coarsening to occur. It was recently implied by Okada *et al.* [40] that the spherical morphology of their off-critical 3D polymer blends caused slower ($d \sim t^{1/3}$) growth, while the interconnected morphology observed in their near-critical blends allowed the accelerated coarsening rates ($d \sim t^1$); however, it should be noted that the morphology may be a result of the accelerated growth rate, and not the other way around. The presence of a circular morphology in our 2D systems as seen in Fig. 2(a) does not prevent flow (as implied by Okada *et al.* [40]); there are wide and narrow regions, and the crossover to a flow regime may be due to the existence of domains large enough to be considered "wide" regions, assuming there is enough dispersed phase (e.g., near-critical system) for there also to be "narrow" regions [41]. Thus a circular morphology may not necessarily prevent a flow mechanism. Similarly, while the unusual morphologies observed in our 2D critical systems [Fig. 2(b)] may have caused very fast growth, it is possible that it is the fast growth which caused the unusual morphologies.

The dependence of the crossover on F_A and gap width is given in Fig. 8. As each of these systems is a 300kPS-DEO solution phase-separated at the same temperature ($T_{PS} = 33^\circ\text{C}$), σ is identical for the three systems. (This is not the case for the systems represented in Fig. 6 where crossover domain size was seen to be a function of quench depth.)

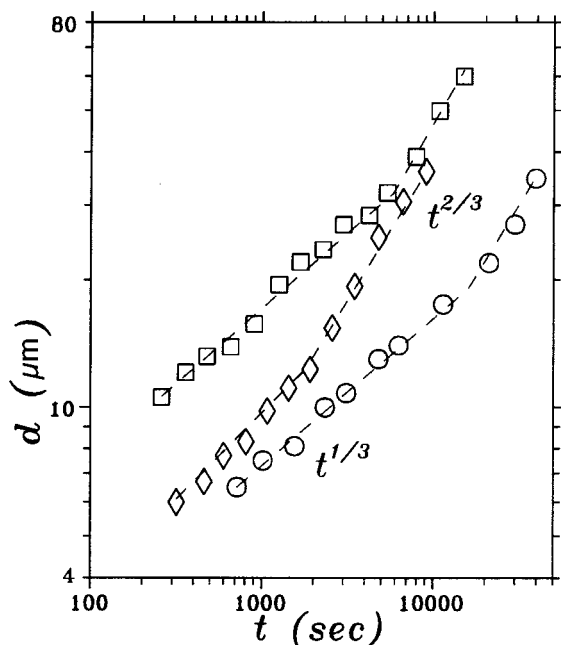


FIG. 8. Temporal dependence of d for near-critical 300kPS-DEO solutions quenched to 33 °C with glass substrates. \diamond : 4 wt %, 10 μm gap, $F_A \sim 0.28$; \square : 5 wt %, 10- μm gap, $F_A \sim 0.35$; \circ : 5 wt %, 1.5- μm gap, $F_A \sim 0.35$. The slopes are not fits, only guides.

At a constant gap width (10 μm), the crossover occurs at a smaller domain size for the 4 wt %, lower F_A system. This dependence of crossover domain size on dispersed-phase area fraction has not yet been considered in any theoretical or numerical study, to our knowledge. A possible explanation for this effect may be the ‘‘availability’’ of flow sites: since σ causes flow from narrow to wide regions, and the lower F_A system would have more wide regions early into the coarsening process, flow may occur at smaller domain size in the system with less dispersed phase. In addition, at constant F_A , a smaller gap width (1.5 vs 10 μm) lowers the crossover domain size; this may be explained by added pressure from the walls. The curvature between the phases schematically shown in Fig. 3(a) would be enhanced for a more narrow gap; this may augment σ effects, causing flow at a smaller domain size.

In order to show the universality of 2D near-critical crossover behavior, domain-size growth rates were determined for several different phase-separating polymer solutions (see Fig. 9). Of these systems, three show crossover behavior: 5 wt % 300kPS-DEO, 2 wt % 2000kPS-DEO, and 2 wt % 2000kPS-DEM. No crossover was observed for any near-critical 300kPS-DIDP system, which could be due to the crossover domain size being larger than the maximum determinable domain size ($\sim 60 \mu\text{m}$) with our experimental setup. (Work is underway to modify equipment to allow determination of larger domain sizes.) The high viscosity of the DIDP system as compared to the DEO and DEM systems does not substantially alter the precrossover growth rate; for the conditions given in Fig. 9, the 300kPS-DIDP system yields $K \approx 1.4 \mu\text{m/s}^{1/3}$, similar to values obtained for the other solvent systems (see the precrossover DEO systems in Fig. 7 as well as the off-critical systems in Fig. 5).

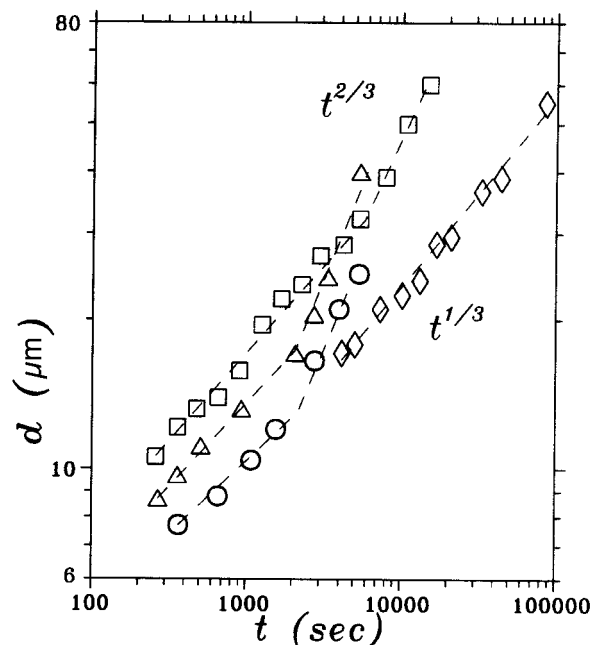


FIG. 9. Temporal dependence of d for near-critical solutions using a 10- μm -gap and glass slides. \square : 5 wt % 300kPS-DEO, $\Delta T = 2^\circ\text{C}$, $F_A \sim 0.35$; \triangle : 2 wt % 2000kPS-DEM, $\Delta T = 1^\circ\text{C}$, $F_A \sim 0.25$; \diamond : 6.5 wt % 300kPS-DIDP, $\Delta T = 2^\circ\text{C}$, $F_A \sim 0.27$; \circ : 2 wt % 2000kPS-DEO, $\Delta T = 1^\circ\text{C}$, $F_A \sim 0.30$. Slopes are not fits, only guides.

Based on interfacial tension effects alone, it is not necessarily expected that the crossover domain size in the 2000kPS-DEO system ($\sim 13 \mu\text{m}$) would be significantly below that of the 300kPS-DEO system ($\sim 30\text{--}35 \mu\text{m}$), as shown in Fig. 9. Since σ decreases with increasing polymer molecular weight [39], the crossover domain size may be expected to be larger in the 2000kPS-DEO system, the opposite of what is observed. The different quench depths employed with the 300kPS-DEO and 2000kPS-DEO systems also might suggest that the higher molecular weight system should have a larger crossover domain size. However, the lower F_A value and crossover domain size of the higher molecular weight system are consistent with the F_A effects observed as a function of composition in Fig. 8. Given that DEO and DEM solutions using the same polymer molecular weight at similar quenches below T_c also reveal substantial differences in crossover domain size, σ measurements for these systems as a function of molecular weight and solvent are very important. In this way, a better understanding of the role of σ in crossover domain size may be obtained.

Comparison with other quantitative, experimental 2D coarsening studies

The studies described above in subsections B and C, extensions of our work in Ref. [19], which reported crossover in domain-size growth rate for 2D near-critical systems, relate to well characterized polymer-solvent systems. Coarsening behavior was monitored at sufficiently long times so that conditions of approximately constant dispersed-phase area fraction (implying that equilibrium phase compositions had been achieved) and thermal equilibrium within the sample are found to hold. This is necessary for a quantitative comparison with theory and numerical simulation studies which

typically assume such conditions. In the case of off-critical and near-critical conditions, these experimental studies substantially confirm either quantitatively (as in the growth-rate exponents) or qualitatively (as in the dependence of the parameter K on F_A for all but one situation) expectations from theory and simulation. As indicated in subsection A above, quantitative analysis of approximately critical systems was not possible in the present study, although apparent growth rates were very high. This is in accord with observations by Bodensohn and Goldburg [20] who, in a two-dimensional coarsening study of a critical mix of two low molecular weight liquids, found that coarsening happened much faster than in a bulk mixture, and that there was no significant time interval over which the domain size grew algebraically with time.

In contrast, there is a limited series of experiments by Tanaka [32,33], using systems related to those of the present study, which deviate significantly from expectations based on conventional phase separation and coarsening theory. In particular, Tanaka [32] recently reported a coarsening growth rate scaling as $t^{0.15}$ for approximately critical PS-DEM systems (with PS of several different molecular weights) and as $t^{0.1}$ for a (polymer-lean) off-critical PS-DEM system. These determinations were not made from direct analysis of domain sizes but from 2D Fourier transforms of digital images, from which a pseudo-structure-factor was determined as a function of wave number. Tanaka claimed that, since the refractive index of a phase is proportional to its brightness in an image [42], this structure factor is directly proportional to the structure factor obtained from scattering studies; therefore, he took the wave number for the peak structure factor (q_m) to be inversely proportional to d [42].

Tanaka attributed this anomalously slow growth rate to a mode of coarsening which he termed “viscoelastic spinodal decomposition” [32,33,43], in direct opposition to Ostwald ripening theories which discuss the “universality” of the growth behavior [11]. Accepting for the moment Tanaka’s general approach for determining the growth-rate exponent, the comparison made by Tanaka between his experimental data and the expectations based on conventional theory and simulation may be questioned on several fronts. First, in the one case where the pseudo-structure-factor is plotted as a function of wave number [32], the peak is shown to be very broad, making the assumption of equivalence between q_m and the *average* domain size, d , tenuous. Furthermore, the time scales represented in the plot showing the temporal change of the pseudo-structure-factor as a function of wave number range from only 1 to 100 s, well below *any* of the time scales used in the studies reported here for determining coarsening growth rates. In fact, none of the data reported by Tanaka exceeds 720 s, and his coarsening data are often shown on time scales of 2, 2.5, 4, 5, and 10 s after quenches of as much as 12 °C, conditions where extreme thermal gradients throughout a sample and rapid changes in average sample temperatures must hold. In some cases [33] involving poly(vinyl methyl ether)–water systems, apparent 2D coarsening results purportedly illustrating a linearity of domain size with coarsening time are obtained from *maximum* coarsening times of only 1–5 s.

This is an important point, since a valid comparison with theory or numerical simulation studies (which assume that

phase compositions have reached equilibrium and that no thermal gradients exist within the sample under study) requires that sufficiently long time scales are employed. This point was also made earlier in the two-dimensional coarsening study by Bodensohn and Goldburg [20]; they indicated that, even for the extremely small quenches of 15 mK below the critical temperature required by their use of a critical, low molecular weight mixture, “the time for the system to reach its final temperature was (about) 25 s, so we were barred from studying the early stages of phase separation.” (Furthermore, when conditions were used in the present study involving very rapid quenching where significant thermal gradients were present in the sample, flow effects similar to those described by Tanaka [32,33] and ascribed to viscoelastic phase separation rather than to the temperature gradients inducing flow, were observed.) In the studies reported in subsections B and C above, the assumption of equilibrium phase compositions was verified by demonstrating constancy of the dispersed-phase area fraction, F_A ; in contrast, F_A constancy was neither verified nor is likely to hold for the conditions reported by Tanaka [32,33].

As a result, it is not surprising that Tanaka’s apparent coarsening growth rates would differ significantly from the expectations based on theory and simulation. It is noteworthy that several other coarsening studies have been reported in the research literature with apparently anomalous growth rates which may actually be consistent with conventional coarsening ideas. For example, while slower-than-predicted growth rates ($\sim t^{0.2}$) have been reported for phase-separated diblock copolymer films [31], these data were later reanalyzed by Ardell [38] who, by focusing on the long-time data, demonstrated that the results were in fact consistent with $d \sim t^{1/3}$. As well, 3D coarsening studies of PS-solvent systems by Song and Torkelson [9,10] yielded apparent domain-size growth-rate exponents in the early stages of coarsening (prior to hydrodynamic flow effects) ranging from as low as 0.05 to $\frac{1}{3}$, depending on the system and quench depth employed (generally lower exponents were obtained for shallower quenches). However, reconsideration of these data [44] suggests that at least some of the anomalously slow coarsening results could be associated with the systems not being at conditions of equilibrium phase compositions, i.e., no confirmation of constant phase volume fractions was attempted as a part of those studies. Thus, while the issues pointed out above in no way invalidate Tanaka’s interesting observations [32,33], it is clear that other options beyond viscoelastic phase separation exist to explain them.

Film thickness and substrate polarity effects

From Fig. 8, gap width is revealed to play a strong role in determining domain size in 2D coarsening of near-critical solutions, with much smaller d values being present with the narrower, 1.5- μm gap-width system. Similar effects are observed for off-critical solutions, and data for both off- and near-critical systems are plotted as functions of $t^{1/3}$ and gap width in Fig. 10. For the near-critical system, Fig. 10 reveals that the parameter K (slope in Fig. 10) is almost a factor of 2 greater for a 10- μm gap than for a 1.5- μm gap; however, K values for the 1.5- and 10- μm gaps for the off-critical systems are very similar. Therefore, the coalescence mechanism

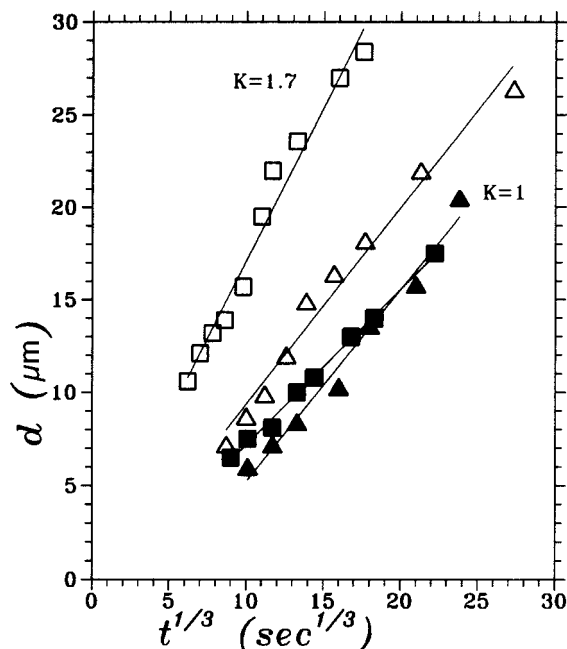


FIG. 10. Plot of d as a function of $t^{1/3}$ for two near-critical (precrossover) and two off-critical 300kPS-DEO solutions comparing effects of gap width. \square : 5.0 wt % (near-critical), $\Delta T=2^\circ\text{C}$, 10- μm gap; \blacksquare : 5.0 wt % (near-critical), $\Delta T=2^\circ\text{C}$, 1.5- μm gap; \triangle : 2.5 wt % (off-critical), $\Delta T=2^\circ\text{C}$, 10- μm gap; \blacktriangle : 2.5 wt % (off-critical), $\Delta T=2^\circ\text{C}$, 1.5- μm gap. Note that the lines are best-fit slopes ($K[=]\mu\text{m}/\text{s}^{1/3}$).

has a greater dependence on gap width than Ostwald ripening, implying that Brownian motion (i.e., the transport mechanism for coalescence) is more hindered by a thinner gap than diffusion (i.e., the one for Ostwald ripening). As gap-width effects in 2D coarsening have not been considered prior to this study, they merit further investigation.

The effect of substrate polarity on coarsening is very different for off- and near-critical systems. Figure 11 shows domain-size growth rates for similar off-critical systems phase separated between either glass or nonpolar slides. These data indicate that off-critical coarsening depends little on substrate; likewise, the domain size and qualitative morphology are affected slightly by substrate polarity. This similarity is expected since changing the substrate only affects the curvature between the phases [see Fig. 3(a)], which should have little effect on the growth rate in an evaporation-condensation mechanism.

In contrast, the resultant morphology and coarsening rate for near-critical systems are significantly affected by substrate. Figure 12 shows micrographs from two 5 wt % 300kPS-DEO systems ($\Delta T=2^\circ\text{C}$) phase separated between either glass or nonpolar slides. Early-time coarsening behavior [Figs. 12(a) and 12(c)] is not affected by substrate. However, once the domains reach a size scale approaching that of the crossover domain size, i.e., when σ becomes important, the domain-size growth rate for the system phase separated between nonpolar substrates increases significantly ($d>t^1$), and the morphology starts to become very unusual [compare Figs. 12(b) and 12(d)]. Once this occurs, the domain-size growth rates become impossible to determine because of

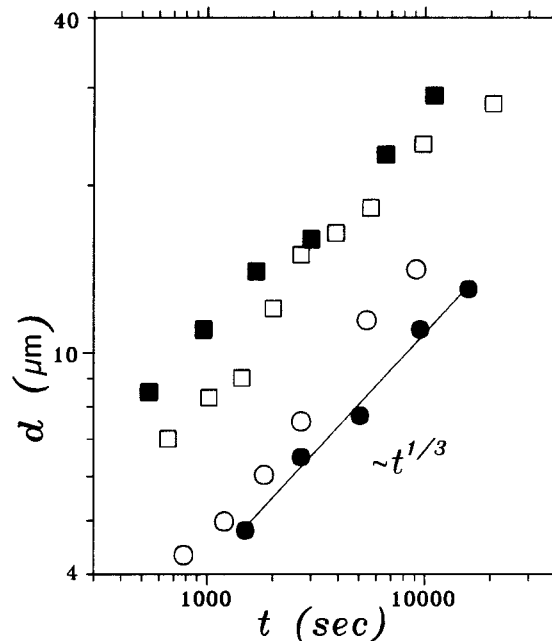


FIG. 11. Temporal dependence of d for off-critical solutions using a 10- μm gap and either glass or nonpolar slides. \square : 2.5 wt % 300kPS-DEO, $\Delta T=2^\circ\text{C}$ (glass); \blacksquare : 2.5 wt % 300kPS-DEO, $\Delta T=2^\circ\text{C}$ (nonpolar); \circ : 1.0 wt % 2000kPS-DEM, $\Delta T=1^\circ\text{C}$ (glass); \bullet : 1.0 wt % 2000kPS-DEM, $\Delta T=1^\circ\text{C}$ (nonpolar).

both the elongated nature of their domains and their accelerated coarsening rates. The unusual morphologies and fast growth rates present in these near-critical nonpolar-substrate systems are similar to critical systems [see Fig. 2(b)], and are probably caused by interfacial tension effects such as added pressure due to the nonpolar walls. When the substrate is polar (glass), it attracts the polar polymer-lean phase more than the less polar polymer-rich phase, causing pressure on only the polymer-rich dispersed phase. However, when the substrate is nonpolar, both phases are repelled by the substrate; therefore, the phases minimize their surface area at a much greater rate due to the added pressure of the walls. This increased coalescence rate does not allow a droplet to reach its desired, energy-minimizing circular form before impingement with another droplet, causing the unusual morphology seen in Fig. 12(d).

CONCLUSIONS

We have reported a comprehensive experimental study of 2D coarsening. With the use of several polymer-solvent systems, the effects of composition (off- and near-critical), quench depth, dispersed-phase area fraction, film thickness, substrate polarity, polymer molecular weight, and solvent viscosity on domain size and domain-size growth rate were studied by optical microscopy over coarsening time scales from several minutes to more than ten hours. For the conditions studied, no significant effect of polymer molecular weight was observed, except to the extent that it defined the shape and location of the phase diagram for each polymer-solvent system.

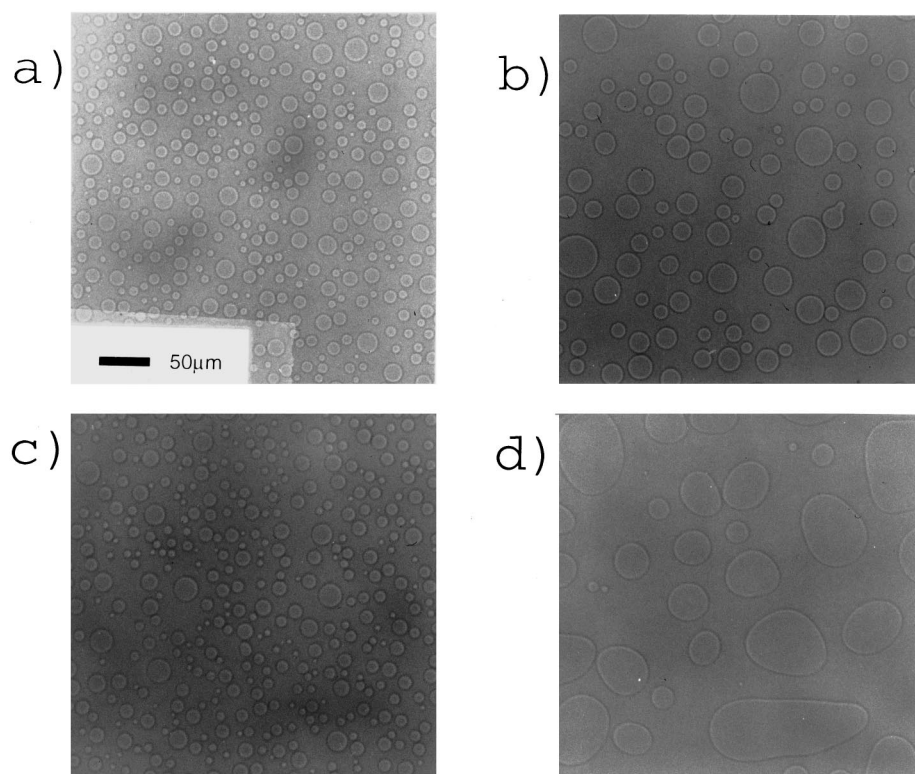


FIG. 12. Optical micrographs for 5 wt % 300kPS-DEO (near-critical) solutions using a 10- μm gap, $\Delta T=2^\circ\text{C}$, between glass or nonpolar slides: (a) between glass, coarsened for 180 s; (b) between glass, coarsened for 1800 s; (c) between nonpolar, coarsened for 210 s; (d) between nonpolar, coarsened for 2280 s. Please note that while the morphologies are regular (i.e., circular) for each substrate at early coarsening times [compare (a) and (c)], noncircular, irregular structures appear between the nonpolar substrates at later times [compare (b) and (d)]. The scale bar is applicable to all four micrographs.

With regard to composition effects, phase-separated off-critical (polymer-lean) solutions coarsened predominantly by evaporation-condensation (Ostwald ripening), with $d=Kt^{1/3}$. The parameter K increased with increasing dispersed-phase area fraction F_A , in qualitative agreement with theory developed for 3D coarsening [11,12]. Near-critical (polymer-lean) coarsening featured much more droplet impingement (coalescence) as well as Ostwald ripening, with $d=Kt^{1/3}$ at early times; at longer times, a crossover to a higher $t^{2/3}$ growth rate was observed for some of the polymer-solvent systems. The domain size at which this crossover occurred decreased with increasing quench depth; this is in qualitative, although not quantitative, agreement with predictions for crossover from thermal- to flow-dominated coarsening in 3D [3].

The growth-rate exponents of $\frac{1}{3}$ and $\frac{2}{3}$ have been determined here with high precision for many cases of coarsening. For off-critical and early-time near-critical coarsening, the best-fit exponents ranged from 0.30 to 0.42, and in each case the domain size could be plotted as a function of $t^{1/3}$, yielding a very good linear dependence. For long-time near-critical coarsening after the crossover to a different coarsening mechanism, best-fit growth-rate exponents ranged from 0.62 to 0.69, and in each case the domain size could be plotted as a function of $t^{2/3}$, also with a very good linear dependence. Thus, this study confirms the theoretical and numerical predictions [12] of a $t^{1/3}$ growth rate for 2D Ostwald ripening, when the dispersed-phase area fraction is small, and the predictions [1,15,18] for an initial $t^{1/3}$ growth rate followed by a crossover to a $t^{2/3}$ growth rate for 2D coarsening in near-critical systems, when the dispersed-phase area fraction is larger.

Other factors being equal, increasing the quench depth

resulted in smaller domain size, at least until a crossover to a $t^{2/3}$ growth rate. This is due to the smaller domain size formed with increasing quench depth in the initial stages of spinodal decomposition [37] prior to the onset of coarsening. With sufficiently large quenches, the dispersed-phase area fraction is a significant function of quench depth due to the asymmetric nature of the polymer-solvent phase diagram, and area fraction effects become important. For near-critical systems the crossover to a $t^{2/3}$ growth rate occurs at a smaller domain size with increasing quench depth; at long times this quench-depth dependence of the crossover can result in larger domain size with greater quench depth.

Finally, with thinner films, the average domain size was significantly smaller over the entire coarsening range for both off- and near-critical systems. This is likely due to slower coarsening in 2D as compared to 3D, with the thinner films entering a condition of 2D coarsening at shorter times, all else being equal. Gap width also affected the K values for the early stage of near-critical coarsening, although off-critical K values were not affected; this suggests that coalescence is more hindered by a thinner gap than Ostwald ripening. Coarsening in off-critical systems depended little on substrate polarity; however, near-critical coarsening near the crossover was strongly affected by substrate. Such effects have not been considered theoretically and merit further study.

ACKNOWLEDGMENTS

We thank Professor Wesley Burghardt for use of his optical microscopy and hot stage. This research was sponsored by NASA-Marshall (Grant No. NAG8-1061).

- [1] H. Furukawa, *Adv. Phys.* **34**, 703 (1985).
- [2] J. D. Gunton, M. San Miguel, and P. Sahni, in *Phase Transformations and Critical Phenomena*, edited by C. Domb and J. Lebowitz (Academic, London, 1983), Vol. 8, p. 267, and references therein.
- [3] J. H. Aubert and R. L. Clough, *Polymer* **26**, 2047 (1985).
- [4] J. Lal and R. Bansil, *Macromolecules* **24**, 290 (1991).
- [5] E. D. Siggia, *Phys. Rev. A* **20**, 595 (1979).
- [6] Y. C. Chou and W. I. Goldburg, *Phys. Rev. A* **20**, 2015 (1979); N.-C. Wong and C. M. Knobler, *J. Chem. Phys.* **69**, 725 (1979).
- [7] T. Kyu and J. M. Saldana, *Macromolecules* **21**, 1021 (1988); M. Takashi, S. Kinoshita, and T. Nose, *J. Polym. Sci. B* **27**, 2159 (1989); S. Nojima, Y. Ohyama, M. Yamaguchi, and T. Nose, *Polym. J.* **14**, 907 (1982); I. G. Voigt-Martin, K.-H. Leister, R. Roseneau, and R. Koningsveld, *J. Polym. Sci. B* **24**, 723 (1986); T. Hashimoto, M. Itakura, and H. Hasegawa, *J. Chem. Phys.* **85**, 6118 (1986); T. Hashimoto, M. Itakura, and N. Shimidzu, *ibid.* **85**, 6773 (1986).
- [8] F. S. Bates and P. Wiltzius, *J. Chem. Phys.* **91**, 3258 (1989).
- [9] S.-W. Song and J. M. Torkelson, *Macromolecules* **27**, 6389 (1994).
- [10] S.-W. Song and J. M. Torkelson, *J. Membr. Sci.* **98**, 209 (1995).
- [11] P. W. Voorhees, *J. Stat. Phys.* **38**, 231 (1985); *Ann. Rev. Mater. Sci.* **22**, 197 (1992).
- [12] J. H. Yao, K. R. Elder, H. Guo, and M. Grant, *Phys. Rev. B* **45**, 8173 (1992); J. H. Yao, K. R. Elder, H. Guo, and M. Grant, *ibid.* **47**, 14 110 (1993); A. Chakrabarti, R. Toral, and J. D. Gunton, *Phys. Rev. E* **47**, 3025 (1993); Q. Zheng and J. D. Gunton, *Phys. Rev. A* **39**, 4848 (1989).
- [13] I. M. Lifshitz and V. V. Slyozov, *J. Phys. Chem. Solids* **19**, 35 (1961).
- [14] E. Velasco and S. J. Toxvaerd, *Phys. Rev. Lett.* **71**, 388 (1993).
- [15] J. E. Farrell and O. T. Valls, *Phys. Rev. B* **40**, 7027 (1989); **42**, 2353 (1990).
- [16] K. Binder and D. Stauffer, *Phys. Rev. Lett.* **33**, 1006 (1974); G. Leptoukh, B. Strickland, and C. Roland, *ibid.* **74**, 3636 (1995).
- [17] H. Furukawa, *Phys. Rev. A* **31**, 1103 (1985); *ibid.* **36**, 2288 (1987); *Physica A* **204**, 237 (1994).
- [18] S. Bastea and J. L. Lebowitz, *Phys. Rev. E* **52**, 3821 (1995); F. J. Alexander, S. Chen, and D. W. Grunau, *Phys. Rev. B* **48**, 634 (1993); Y. Wu, F. J. Alexander, T. Lookman, and S. Chen, *Phys. Rev. Lett.* **74**, 3852 (1995).
- [19] C. K. Haas and J. M. Torkelson, *Phys. Rev. Lett.* **75**, 3134 (1995).
- [20] J. Bodensohn and W. I. Goldburg, *Phys. Rev. A* **46**, 5084 (1992).
- [21] L. Sung, A. Karim, J. F. Douglas, and C. C. Han, *Phys. Rev. Lett.* **76**, 4368 (1996).
- [22] E. Velasco and S. Toxvaerd, *Phys. Rev. E* **54**, 605 (1996).
- [23] T. Lookman, Y. Wu, F. J. Alexander, and S. Chen, *Phys. Rev. E* **53**, 5513 (1996).
- [24] M. R. Moldover and J. W. Cahn, *Science* **207**, 1075 (1980); J. W. Cahn, *J. Chem. Phys.* **66**, 3667 (1977).
- [25] T. Hashimoto, *Phase Transitions* **12**, 47 (1988); D.-W. Park and R.-J. Roe, *Macromolecules* **24**, 5324 (1991); M. He, Y. Liu, Y. Feng, M. Jiang, and C. C. Han, *ibid.* **24**, 464 (1991); M. Okada, J. Sun, J. Tao, T. Chiba, and T. Nose, *ibid.* **28**, 7514 (1995); B. Crist and A. Nesarikar, *ibid.* **28**, 890 (1995).
- [26] K. Kubota and N. Kuwahara, *Phys. Rev. Lett.* **68**, 197 (1992); N. Kuwahara, M. Tachikawa, K. Hamano, and Y. Kenmochi, *Phys. Rev. A* **25**, 3449 (1982).
- [27] K. S. McGuire, A. Laxminarayan, and D. R. Lloyd, *Polymer* **36**, 4951 (1995).
- [28] S. Nojima, K. Shiroshita, and T. Nose, *Polym. J.* **14**, 289 (1982).
- [29] S.-W. Song, Ph.D. dissertation, Northwestern University, 1994.
- [30] W. R. White and P. Wiltzius, *Phys. Rev. Lett.* **75**, 3012 (1995).
- [31] P. Bassereau, D. Brodbeck, T. P. Russell, H. R. Brown, and K. R. Shull, *Phys. Rev. Lett.* **71**, 1716 (1993).
- [32] H. Tanaka, *Phys. Rev. Lett.* **71**, 3158 (1993).
- [33] H. Tanaka, *Phys. Rev. Lett.* **70**, 2770 (1993); *Macromolecules* **25**, 6377 (1992).
- [34] F.-J. Tsai and J. M. Torkelson, *Macromolecules* **21**, 1026 (1988).
- [35] B. Lom, K. E. Healy, and P. E. Hockberger, *J. Neurosci. Meth.* **50**, 385 (1994).
- [36] *Solvents Safety Handbook*, edited by D. J. de Renzo (Noyes Data Corp., Park Ridge, NJ, 1986).
- [37] J. W. Cahn, *Trans. Metall. Soc. AIME* **242**, 166 (1968); J. W. Cahn and J. E. Hilliard, *J. Chem. Phys.* **31**, 688 (1959).
- [38] A. J. Ardell, *Phys. Rev. Lett.* **74**, 4960 (1995).
- [39] K.-Q. Xia, C. Franck, and B. Widom, *J. Chem. Phys.* **97**, 1446 (1992); K. Shinozaki, T. V. Tan, Y. Saito, and T. Nose, *J. Chem. Phys.* **23**, 728 (1982).
- [40] M. Okada, J. Sun, J. Tao, T. Chiba, and T. Nose, *Macromolecules* **28**, 7514 (1995).
- [41] To clarify this point, a pipe analogy will be used to describe hydrodynamic flow. Matrix-phase (i.e., continuous phase) material features “narrow” regions (i.e., areas between two droplets which are spatially close) and “wide” regions (i.e., relatively large spaces where no droplets are present). The narrow regions are comparable to small-diameter pipes and feel a higher pressure due to σ effects than will the wide regions. Therefore, matrix-phase material flows from areas of high pressure to low pressure, similar to flows in a network of different-sized pipes.
- [42] H. Tanaka, T. Hayashi, and T. Nishi, *J. Appl. Phys.* **59**, 3627 (1986); **65**, 4480 (1989).
- [43] H. Tanaka, *Phys. Rev. Lett.* **72**, 1702 (1994); *J. Chem. Phys.* **100**, 5323 (1994).
- [44] C. K. Haas and J. M. Torkelson (unpublished).